



Magnetic and structural properties of the chromium-based $\text{Mn}_{1-x}\text{Cd}_x\text{Cr}_2\text{S}_4$ thiospinel

Patricia Barahona^{a,*}, Antonio Galdamez^b, Víctor Manríquez^b, Octavio Peña^c

^a Instituto de Ciencias Básicas, Universidad Católica del Maule, Talca, Chile

^b Departamento de Química, Facultad de Ciencias, Universidad de Chile, Santiago, Chile

^c Sciences Chimiques de Rennes, UMR 6226, Université de Rennes 1, Rennes, France

ARTICLE INFO

Article history:

Received 5 February 2009

Accepted 21 February 2009

Available online 9 March 2009

Keywords:

Ferrimagnetic perovskites

Spin reversal

Cooperative phenomena

ABSTRACT

The $(\text{Mn}_{1-x}\text{Cd}_x)\text{Cr}_2\text{S}_4$ phases ($0 \leq x \leq 0.6$) have been synthesized from the corresponding elements at 1123 K. These samples were characterized by powder X-ray diffraction (XRD) and magnetic susceptibility. The $(\text{Mn}_{1-x}\text{Cd}_x)\text{Cr}_2\text{S}_4$ compounds crystallize in the space group $Fd-3m$ with cell parameters $a = 10.101(6)$ Å, $10.139(3)$ Å, $10.165(2)$ Å, and $10.192(1)$ Å for $x = 0, 0.2, 0.4$ and 0.6 , respectively. An overall ferrimagnetic behavior is observed for all samples. The ferromagnetic component increases rapidly when manganese is substituted by non-magnetic cadmium, as shown by ZFC/FC measurements. At the same time, the value of the magnetization M_{50} at 50 kOe, deduced from $M(H)$ loops, also increases with increasing cadmium content because the antiferromagnetic alignment between chromium and manganese spins is progressively lost, leading toward well aligned moments pointing into the same direction. These results are explained by a rearrangement of the chromium spins when Mn located at the tetrahedral sites, is substituted by Cd.

© 2009 Elsevier B.V. All rights reserved.

1. Introduction

The discovery of the colossal magneto-resistance CMR effect has attracted a renewed interest in manganites perovskites LnMnO_3 (Ln = lanthanide) partially substituted at the A-site by an alkaline earth metal, $\text{Ln}_{1-x}\text{A}_x\text{MnO}_3$, due to their potential technological applications in the manufacture of electronic devices [1–3]. The essential physical mechanisms of the CMR phenomenon in these manganites are believed to be the double-exchange (DE) and Jahn–Teller (JT) effects, both intimately related to the mixed-valence character of the Mn cation [4]. However, in chromium-based chalcogenide materials of spinel structure ACr_2S_4 (A = transition metal), also identified as CMR materials, there are neither heterovalence nor JT effect [5]. Thus, it becomes very interesting to look deeper onto the magnetic ordering and the interaction mechanisms which might exist between the two (or more) magnetic sublattices coexisting in the spinel structure.

The magnetic and transport properties in chalcogenide spinels ACr_2S_4 are strongly influenced by the distribution of the metal ions in the structure. This is essentially related to (i) the existence of two types of cationic sites, tetrahedral (A) and octahedral (B); and (ii) the great flexibility of the structure in hosting various metal ions, differently distributed between sites, with a large possibility of sub-

stitution between them. As the cationic distribution can change when substitution occurs, the physical properties of the spinel material may strongly differ from those of the non-substituted compound. Therefore, solid solutions of thiospinels have received considerable attention for their interesting electrical and magnetic properties, which can greatly vary as a function of composition [6,7].

The chalcogenide spinel MnCr_2S_4 crystallizes in a normal spinel structure (space group $Fd-3m$), in which Mn and Cr ions occupy the tetrahedral A and octahedral B sites, respectively. In this paper, we report mixed-cation phases $(\text{Mn}_{1-x}\text{Cd}_x)\text{Cr}_2\text{S}_4$ ($x = 0.2, 0.4$ and 0.6) where manganese is partially substituted by cadmium in the ferrimagnetic compound MnCr_2S_4 . The non-substituted MnCr_2S_4 compound was prepared under the same synthesis procedure, and results are reported for comparison. The aim of this work is to study the influence of the substitution in the A-site by non-magnetic Cd^{2+} ion onto the magnetic properties of the MnCr_2S_4 thiospinel.

2. Experimental

To prepare the $(\text{Mn}_{1-x}\text{Cd}_x)\text{Cr}_2\text{S}_4$ phases ($0 \leq x \leq 0.6$), high-purity powders of the corresponding elements (99.99%) were mixed in stoichiometric amounts, sealed in evacuated quartz tubes using I_2 as transport agent. The tubes were slowly heated from ambient temperature to 1073 K at a rate of 5 K/min and held at maximum temperature over a period of 1 week. Subsequently, the resultant was reground and fired again at 1123 K for 3 days.

The X-ray diffraction (XRD) powder data were collected at room temperature on a Siemens D 5000 diffractometer, with Cu K_α radiation, in the range $5^\circ \leq 2\theta \leq 80^\circ$. The lattice parameters were calculated from least-square fits using the powder diffraction package (PDP) [8] and powder pattern lattice parameter (PPLP) refinement

* Corresponding author. Tel.: +56 71 203 161; fax: +56 71 203 667.

E-mail address: pbaraho@ucm.cl (P. Barahona).

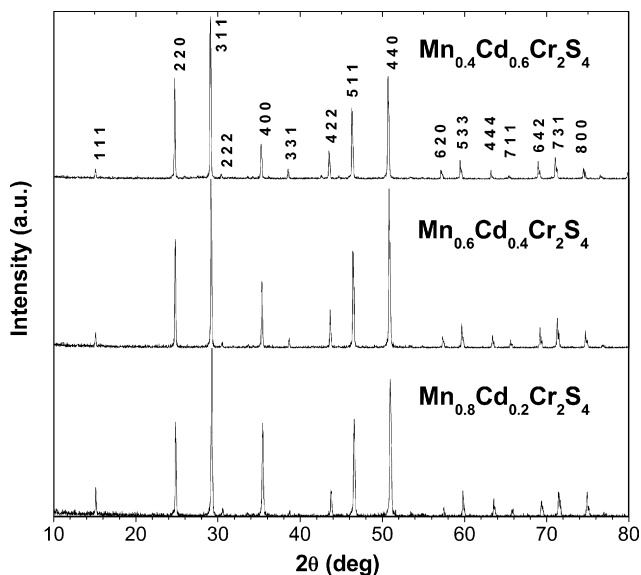


Fig. 1. XRD patterns of $\text{Mn}_{0.8}\text{Cd}_{0.2}\text{Cr}_2\text{S}_4$, $\text{Mn}_{0.6}\text{Cd}_{0.4}\text{Cr}_2\text{S}_4$ and $\text{Mn}_{0.4}\text{Cd}_{0.6}\text{Cr}_2\text{S}_4$.

routine of the NRCVAX program [9]. EDX analyses, performed on a JEOL 6400 Scanning electron microscope equipped with Oxford Link Isis energy dispersive X-ray (EDX) detector, showed a good agreement (within 5%) with the expected compositions.

Magnetic measurements were performed using a Quantum Design MPMS-XL5 SQUID magnetometer between 2 and 400 K, under different applied fields (10 kOe for measurements above T_c and 100 Oe for ZFC/FC cycles). Magnetization loops $M(H)$ between -50 and $+50$ kOe were measured at 2 K. Powder samples were pelletized, placed inside a gelatin capsule and held tightly in order to avoid any re-orientation with respect to the external field; a small drop of vacuum grease, of negligible diamagnetic contribution compared to the specimens' signal, helped to freeze the crystallites into random positions when in the low temperature ordered state.

3. Results and discussion

3.1. X-ray diffraction results

The XRD measurements of the $(\text{Mn}_{1-x}\text{Cd}_x)\text{Cr}_2\text{S}_4$ phases ($x = 0.2, 0.4$ and 0.6) show sharp lines that reflect the good crystallinity and homogeneity of the prepared samples (Fig. 1). The substitution of manganese by cadmium in $(\text{Mn,Cd})\text{Cr}_2\text{S}_4$ results in crystalline phases with structures identical to the one of MnCr_2S_4 [10]. No secondary phases were observed, in the limit of the experimental detection of both SEM–EDX and XRD analyses (less than 5% for both techniques).

Table 1

Powder diffraction data of $\text{Mn}_{1-x}\text{Cd}_x\text{Cr}_2\text{S}_4$ ($x = 0.2, 0.4, 0.6$).

$\text{Mn}_{0.8}\text{Cd}_{0.2}\text{Cr}_2\text{S}_4$				$\text{Mn}_{0.6}\text{Cd}_{0.4}\text{Cr}_2\text{S}_4$				$\text{Mn}_{0.4}\text{Cd}_{0.6}\text{Cr}_2\text{S}_4$			
hkl	d_{obs}	d_{calc}	I_{rel}	hkl	d_{obs}	d_{calc}	I_{rel}	hkl	d_{obs}	d_{calc}	I_{rel}
111	5.853	5.850	13	111	5.860	5.870	8	111	5.860	5.880	4
220	3.580	3.585	41	220	3.590	3.594	56	220	3.594	3.603	62
311	3.049	3.057	100	311	3.061	3.065	100	311	3.067	3.073	100
222	2.922	2.927	4	222	2.924	2.934	3	222	2.939	2.942	3
400	2.530	2.535	41	400	2.538	2.541	34	400	2.544	2.548	22
331	2.323	2.326	3	331	2.326	2.332	5	331	2.333	2.338	6
422	2.067	2.070	12	422	2.073	2.075	20	422	2.078	2.080	17
511	1.948	1.951	43	511	1.954	1.956	50	511	1.959	1.961	44
440	1.791	1.792	60	440	1.795	1.797	82	440	1.799	1.802	63
620	1.601	1.603	4	620	1.605	1.607	6	620	1.611	1.611	7
533	1.545	1.546	11	533	1.549	1.550	13	533	1.553	1.554	12
444	1.462	1.464	8	444	1.465	1.467	7	444	1.469	1.471	5
711	1.416	1.420	3	711	1.421	1.423	5	711	1.426	1.427	2
642	1.354	1.355	7	642	1.357	1.358	11	642	1.360	1.362	11
731	1.320	1.320	11	731	1.322	1.323	15	731	1.325	1.327	13
800	1.266	1.267	11	800	1.269	1.271	9	800	1.272	1.274	7

The XRD patterns of the substituted compounds were fully indexed in the space group $Fd\bar{3}m$. The Miller's indices, the d spacing, and the intensities of the substituted compounds are listed in Table 1. The values of the cell parameter a are given in Table 2. The a parameter, related to the non-substituted compound MnCr_2S_4 ($a = 10.129$ Å for polycrystalline specimens [10], 10.116 Å for single crystals [11], 10.101 Å in this work), increases linearly when cadmium replaces part of manganese in $\text{Mn}_{1-x}\text{Cd}_x\text{Cr}_2\text{S}_4$, as expected from the larger ionic radius of cadmium compared to the one of divalent manganese (Cd^{2+} : 0.92 Å; Mn^{2+} : 0.80 Å) [12].

3.2. Magnetic results

Previous to the discussion of the magnetic behavior of the $\text{Mn}_{1-x}\text{Cd}_x\text{Cr}_2\text{S}_4$ ($x = 0.2, 0.4, 0.6$) phases, it is worth to comment on the results reported on single crystals of non-substituted MnCr_2S_4 [11]. Two magnetic transitions were reported for this compound [11,13]: at $T_c \sim 65$ K, a transition from a paramagnetic to a ferrimagnetic state (Néel collinear structure), followed by a second one at $T_{Y-K} \sim 5$ K to a triangular configuration (non-collinear Yafet–Kittel type). A non-monotonic variation of the field-cooled magnetization M^{FC} showed an increase of M^{FC} when cooling the collinear structure down to $T_{\text{max}} = 42$ K, followed by a decrease of M^{FC} below T_{max} . This apparent maximum is due to an antiferromagnetic alignment of the Mn moments with respect to the Cr sublattice [11,14]. Concomitant to this, such spin re-arrangement results into a non-monotonous increase of the slope of the magnetization $M(H)$ when increasing the applied field, reaching a saturation of about $6 \mu_B$ at extremely high fields (~ 300 kOe) when the Cr moments are fully aligned, while the Mn spins are oriented perpendicular [15,16].

3.3. Paramagnetic state of the $(\text{Mn,Cd})\text{Cr}_2\text{S}_4$ series

The paramagnetic regime was measured at high fields (10 kOe), well above the magnetic transition temperature. The inverse susceptibility was fitted by a classical Curie–Weiss relation $\chi = C/(T - \Theta)$ in the range $1.5 \times T_c \leq T \leq 400$ K, from which the effective moment μ_{eff} and the Curie–Weiss temperature Θ were obtained (Table 2). The effective moment agrees with what can be expected for Mn^{2+} and Cr^{3+} free-spin values, taking as an average moment for the Mn ion a value of $5.7 \mu_B$, as we have shown in Ref. [17]. This assumption is also in agreement with values reported ($7.75 \mu_B$) for polycrystalline samples of MnCr_2S_4 in the high temperature regime ($T > 400$ K) [13]. This result shows a progressive evolution of the magnetic moment in the paramagnetic state when substituting magnetic manganese by non-magnetic cadmium.

Table 2
Crystallographic and magnetic data for the solid solution $\text{Mn}_{1-x}\text{Cd}_x\text{Cr}_2\text{S}_4$. Space group $Fd-3m$.

Compound	a (Å)	$\mu_{\text{eff}} \pm 0.07$ (μ_B)	$\Theta \pm 5$ K (K)	$T_c \pm 1$ K (K)	$M(50 \text{ kOe}, 2 \text{ K})$ (μ_B)
MnCr_2S_4	10.101 (6)	7.41	+30	65	1.72
$\text{Mn}_{0.8}\text{Cd}_{0.2}\text{Cr}_2\text{S}_4$	10.139 (3)	7.07	+53	68	2.06
$\text{Mn}_{0.6}\text{Cd}_{0.4}\text{Cr}_2\text{S}_4$	10.165 (2)	6.58	+69	72	2.82
$\text{Mn}_{0.4}\text{Cd}_{0.6}\text{Cr}_2\text{S}_4$	10.192 (1)	5.96	+91	79	3.45

3.4. Ordered state of the $(\text{Mn,Cd})\text{Cr}_2\text{S}_4$ series

The ordered regime was investigated through ZFC/FC magnetization cycles performed under low applied fields H_{app} (50–100 Oe). Samples were first cooled under no magnetic field and then warmed from 2 up to 300 K under the applied field H_{app} (ZFC mode). Once at the paramagnetic state, samples were then cooled under H_{app} down to the lowest temperature of 2 K (FC mode). Experimental results obtained in polycrystalline samples of MnCr_2S_4 prepared in this work (shown in Fig. 2 for completeness) compare well with reported data ($T_c = 65$ K, $T_{\text{max}} \sim 42$ K and $T_{Y-K} \sim 5$ K) for a single crystal specimen [11]. In our case, we define the paramagnetic-to-ferrimagnetic transition T_c at the temperature of irreversibility between the ZFC and FC modes, that is $T_c = 65 (\pm 1)$ K, while $T_{\text{max}} \sim 32 (\pm 5)$ K relates to the maximum value of the M^{FC} magnetization. According to Ref. [11], T_{max} corresponds to a reorientation of the manganese spins in the presence of the internal field set up by the ferromagnetic chromium sublattice. At lower temperature, at about 5 K, a marked anomaly is seen in both the ZFC and FC magnetizations which corresponds to the Yafet-Kittel type transition from the collinear (above T_{Y-K}) to the non-collinear (below T_{Y-K}) magnetic structure. Thus our data in a polycrystalline sample of MnCr_2S_4 agrees perfectly well with the data obtained in single-crystal specimens, except for the value of T_{max} . A precise evaluation of T_{max} is however, subjected to caution since the thermal variation of M^{FC} is relatively flat in the range ($20 \text{ K} < T < 40 \text{ K}$).

All solid solutions of the $(\text{Mn}_{1-x}\text{Cd}_x)\text{Cr}_2\text{S}_4$ substituted series ($x = 0.2, 0.4$ and 0.6) show a reversible pathway in the paramagnetic state (Fig. 2), with a pronounced upturn at the approach of the magnetic transition temperature T_c (T_c defined as the temperature of irreversibility T_{rev} ; see above). The transition temperatures T_c are given in Table 2, and show a slow but definite evolution with the cadmium content $x(\text{Cd})$, following the same trend as the ferromagnetic interaction parameter Θ .

The zero-field-cooled magnetizations M^{ZFC} (open symbols in Fig. 2) are quite similar in all substituted samples, showing a slight increase with increasing temperature. It is also to be noticed that

the field-cooled magnetization M^{FC} (filled symbols) for $x(\text{Cd}) = 0.2$ shows a slight temperature dependence in the ordered state, as seen by the small decrease with decreasing temperature, which becomes negligible (i.e. M^{FC} becomes flat) for $x(\text{Cd}) = 0.4$ and 0.6 . At the same time, the extrapolation at $T = 0$ of both M^{ZFC} and M^{FC} increases with increasing content of cadmium. All these features indicate stronger ferromagnetism when manganese is being substituted by cadmium and, since cadmium is a diamagnetic component, it suggests that the antiferromagnetic interactions between the Mn and Cr sublattices become weaker, leading toward well aligned spins pointing into the same direction. This argument allows explaining the fact that T_{max} becomes less visible and that the T_{Y-K} transition is not noticed in the substituted samples, within our experimental range of temperatures. Indeed, the antiferromagnetic non-collinear alignment of Mn moments disappears progressively, favoring the ferromagnetic orientation in a collinear configuration. Following the idea of Refs. [11,13,18], we believe that the FC magnetization is due mainly to the ferromagnetic alignment of the Cr moments while the antiferromagnetic contribution of the manganese sublattice gets weaker because, from one side, there are less Mn atoms in the sample and, on the other side, the internal field due to the Cr network imposes a predominant orientation in the direction of the applied field. It is to be noticed that the M^{FC} behavior of the substituted samples is quite different from the one observed in the undoped compound MnCr_2S_4 meaning that the internal field of the Cr sublattice is already very strong when 20 at.% (or more) of the manganese network is being substituted by cadmium, so that the antiferromagnetic alignment between Mn and Cr spins is rapidly lost.

Another way to characterize the ordered state is through magnetization cycles $M(H)$ as a function of the applied field. Fig. 3 shows the data obtained at $T = 2$ K. A strong ferromagnetic component is observed for all samples, characterized by a fast increase of the magnetization for applied fields lower than 2 kOe. At higher fields, the magnetization tends to stabilize or it increases very slowly up to our maximum applied field of +50 kOe. One way to compare all samples

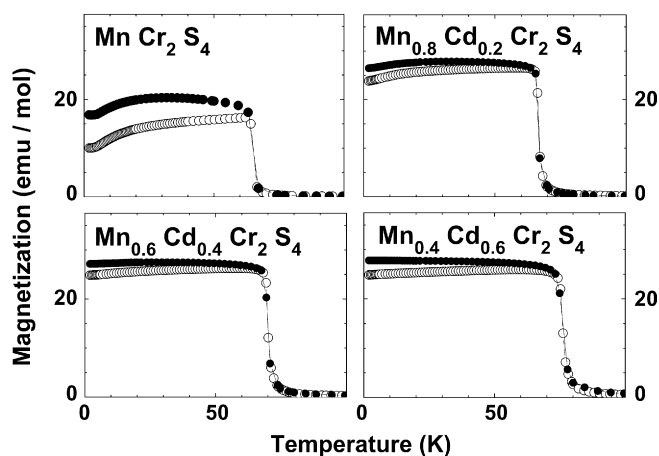


Fig. 2. ZFC/FC magnetization cycles for given solid solutions (ZFC: open symbols; FC: filled symbols).

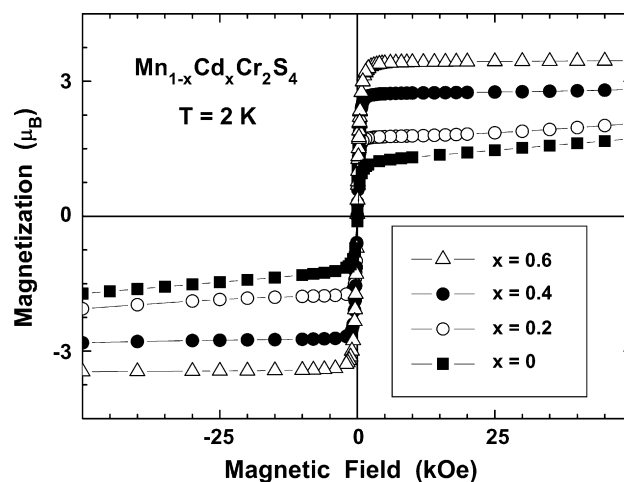


Fig. 3. Magnetization loops measured at $T = 2$ K. Notice the slight upturn at approximately 20 kOe for the $\text{Mn}_{0.8}\text{Cd}_{0.2}\text{Cr}_2\text{S}_4$ sample.

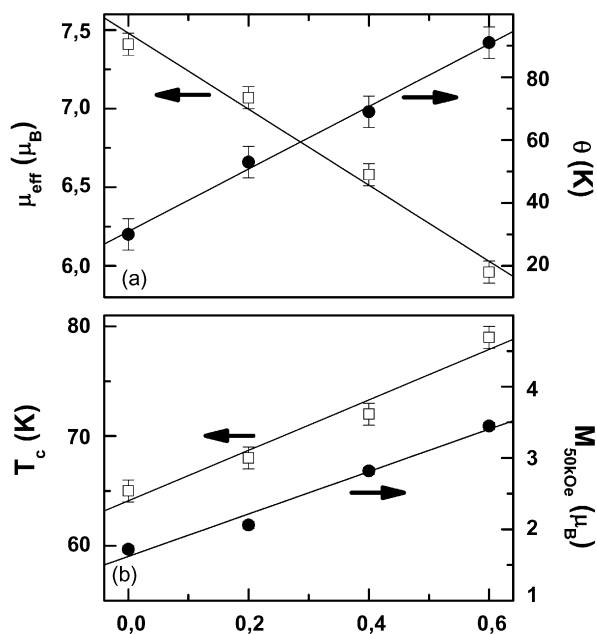


Fig. 4. Magnetic parameters for the solid solution $Mn_{1-x}Cd_xCr_2S_4$, obtained: (a) in the paramagnetic state (μ_{eff} and θ); (b) in the ordered state (T_c and M_{50kOe}).

is to plot the value of the magnetization, $M(50\text{ kOe})$, at the highest experimental field, as a function of the cadmium content, as shown in Fig. 4. The value $M(50\text{ kOe})$ rapidly increases with increasing content of cadmium, indicating again that the antiferromagnetic alignment is progressively lost leading toward well aligned spins pointing into the same direction. This interpretation is confirmed by the field dependence of the magnetization for the $Mn_{0.8}Cd_{0.2}Cr_2S_4$ sample, where a slight upturn of the magnetization is observed in Fig. 3 at approximately 20 kOe, indicating a spin reorientation from a non-collinear toward a collinear magnetic structure. Indeed, as discussed above, an abrupt change in the magnetization slope was observed at a threshold field of 100 kOe in polycrystalline samples of $MnCr_2S_4$ [15] and at lower fields (10–30 kOe) in single crystals (oriented along the $\langle 111 \rangle$ direction) [11]. In our case, the spin reorientation occurs at about 20 kOe in polycrystalline $Mn_{0.8}Cd_{0.2}Cr_2S_4$, confirming that the internal field of the chromium network gets very strong as soon as a small portion of the Mn ions is being substituted. Additional experiments are in progress at much higher applied fields in order to investigate the dependence of the threshold value with the cadmium content and with temperature.

Finally, Fig. 4 summarizes all magnetic data obtained in this work, for both the paramagnetic state (μ_{eff} and θ , Fig. 4a) and ordered state (T_c and M_{50kOe} , Fig. 4b). Quite linear variations are observed in all cases, confirming that the substitution of manganese by cadmium takes place at the same crystallographic site

(tetrahedral A-site) of the normal spinel structure, and that the spin re-arrangement is produced by the progressive substitution of magnetic manganese, antiferromagnetically oriented with respect to the ferromagnetic chromium sublattice, by non-magnetic cadmium.

4. Conclusions

We have investigated the effects of the partial substitution of manganese by cadmium on the structural and magnetic properties of $MnCr_2S_4$. We found that the synthesized compounds $Mn_{1-x}Cd_xCr_2S_4$ ($x=0, 0.2, 0.4, 0.6$) are perfectly homogeneous and they all index in the space group $Fd-3m$. The variation of the lattice parameter is in perfect agreement with the ionic radius of the substituting element.

The ZFC/FC and $M(H)$ magnetization cycles on $Mn_{1-x}Cd_xCr_2S_4$ ($x=0.2, 0.4, 0.6$) show an increase of the ferromagnetic interaction with respect to the ferrimagnetic compound $MnCr_2S_4$, when the cadmium content increases. The antiferromagnetic alignment between Mn and Cr spins is rapidly lost due to the magnetic dilution of the Mn sublattice. In addition, the Cr network imposes a predominant orientation in the direction of the applied field even when a small percentage of Mn (20 at.% or less) is substituted, leading to an important increase of the overall ferromagnetic alignment.

Acknowledgment

Research financed by grant FONDECYT no. 11060462.

References

- [1] R. Von Helmolt, J. Wecker, B. Holzapfel, L. Schultz, K. Samwer, Phys. Rev. Lett. 71 (1993) 2331.
- [2] C.N.R. Rao, B. Raveau (Eds.), Colossal Magnetoresistance Charge Ordering and Related Properties of Manganese Oxides, World Scientific, Singapore, 1998.
- [3] Y. Tokura, Colossal Magnetoresistive Oxides, Gordon & Breach, New York, 2000.
- [4] A.J. Millis, P.B. Littlewood, B.I. Shraiman, Phys. Rev. Lett. 74 (1995) 5144.
- [5] A.P. Ramirez, R.J. Cava, J. Krajewski, Nature 386 (1997) 156.
- [6] A.I. Abramovich, L.I. Koreleva, L.N. Lukina, Phys. Solid State 41 (1999) 73.
- [7] L.I. Koroleva, Y.A. Kessler, L.N. Lukina, T.V. Virovets, D.S. Filimonov, J. Magn. Magn. Mater. 157/158 (1996) 475.
- [8] M. Calligaris, S. Geremias, Powder Diffraction Package, version 3.3, Dipartimento di Scienze, Chimiche Università di Trieste, Italy, 1990.
- [9] A.C. Larson, F.L. Lee, Y.L. Page, M. Webster, J.P. Charland, E.I. Gabe, P.S. White, NRC-VAX Crystal Structure System, Chemistry Division, National Research Council of Canada, Ottawa, Canada, 1987.
- [10] F.K. Lotgering, Philips Res. Rep. 11 (1956) 190.
- [11] V. Tsurkan, M. Mücksch, V. Fritsch, J. Hemberger, M. Klemm, S. Klimm, S. Körner, H.-A. Krug von Nidda, D. Samusi, E.-W. Scheidt, A. Loidl, S. Horn, R. Tidecks, Phys. Rev. B 68 (2003) 134434.
- [12] R.D. Shannon, Acta Crystallogr. A 32 (1976) 751.
- [13] F.K. Lotgering, J. Phys. Chem. Solids 29 (1968) 2193.
- [14] N. Menyuk, K. Dwight, A. Wold, J. Appl. Phys. 36 (1965) 1088.
- [15] J. Denis, Y. Allain, R. Plumier, J. Appl. Phys. 41 (1970) 1091.
- [16] R. Plumier, J. Phys. Chem. Solids 41 (1980) 871.
- [17] P. Barahona, J. Llanos, O. Peña, J. Mater. Chem. 16 (2006) 1567.
- [18] S. Wang, Y. Sun, W. Song, K. Li, Y. Zhang, J. Magn. Magn. Mater. 223 (2001) 238.